

1 **Running title:** OCP-based light sensor

2 **Title:** A synthetic switch based on orange carotenoid protein to control blue light responses in
3 chloroplasts

4 Luca Piccinini¹, Stefano Cazzaniga², Sergio Iacopino³, Matteo Ballottari², Beatrice Giuntoli^{1,3} and
5 Francesco Licausi^{3,4}

6 ¹ Plantlab, Institute of Life Sciences, Scuola Superiore Sant'Anna, Piazza Martiri della Libertà 33, 56127,
7 Pis, Italy

8 ² Department of Biotechnology, University of Verona, Cà Vignal 1, Strada Le Grazie 15, 37134 Verona

9 ³ Department of Biology, University of Pisa, Via Luca Ghini 13, 56126, Pisa, Italy

10 ⁴ Department of Plant Sciences, University of Oxford, South Parks Road, OX1 3RB, Oxford, UK

11 **Author Contributions**

12 B.G., F.L. and L.P. conceived the project design and testing strategy; M. B., B.G., F.L. and S. . supervised
13 the experiments; L.P. generated and analysed transgenic plants, cloned the construct and tested them,
14 S.C. conducted the carotenoid analyses, and S.I. modelled protein structures; A.B. designed the
15 experiments and analyzed the data; L.P., B. G. and F. L. wrote the article with contributions of all the
16 authors. F.L. agrees to serve as the author responsible for contact and ensures communication.

17 **One-sentence summary**

18 Inspired by the light-driven conformational transitions of orange carotenoid proteins of cyanobacteria,
19 we generated a molecular device able to switch its dimeric state in response to blue light.

20

21 **ABSTRACT**

22 Synthetic biology approaches to engineer light-responsive system are widely used, but their applications
23 in plants are still limited, due to the interference with endogenous photoreceptors. Cyanobacteria, such
24 as *Synechocystis spp.*, possess a soluble carotenoid associated protein named Orange Carotenoid
25 binding Protein (OCP) that, when activated by blue-green light, undergoes reversible conformational
26 changes that enable photoprotection of the phycobilisomes. Exploiting this system, we developed a new
27 chloroplast-localized synthetic photoswitch based on a photoreceptor-associated protein-fragment
28 complementation assay (PCA). Since *Arabidopsis thaliana* does not possess the prosthetic group needed
29 for the assembly of the OCP2 protein, we implemented the carotenoid biosynthetic pathway with a
30 bacterial β -carotene ketolase enzyme (*crtW*), to generate keto-carotenoids producing plants. The novel
31 photoswitch was tested and characterized in *Arabidopsis* protoplasts with experiments aimed to
32 uncover its regulation by light intensity, wavelength, and its conversion dynamics. We believe that this
33 pioneer study establishes the basis for future implementation of plastid optogenetics to regulate
34 organelle responses, such as gene transcription or enzymatic activity, upon exposure to specific light
35 spectra.

36

37 **INTRODUCTION**

38 Synthetic biology research applies engineering principles to a multidisciplinary approach to decompose
39 natural systems into their essential components and reassemble them to produce novel functions
40 (Gutmann, 2011). Typically, this is aimed at attaining specific applications but can also serve the purpose
41 of understanding naturally occurring biological devices. The synthetic biology framework often taps
42 from (bio)chemistry, genetics and physics to design and assemble biological constructs in an iterative
43 test and optimize process. Due to their modular nature, genes, proteins and metabolites offer a
44 smorgasbord of opportunities, which is mainly limited by the knowledge or predictability of their
45 structure and function, and the possibility to test them. Among the numerous strands of synthetic
46 biology, a particularly prolific area of research concerns the engineering of photoreactive proteins with
47 signaling potential, such as photoreceptors (Olson and Tabor, 2014). Indeed, light quality and quantity,
48 and their dynamics, provide valuable information for cells to integrate with other exogenous and
49 endogenous cues and respond accordingly. Several chimeric constructs have been developed so far,

50 with a focus on the control of neuronal activity by light, thus establishing the field of optogenetics
51 ('Method of the Year 2010', 2011).

52 Light is essential for photosynthetic organisms and thus impacts most of their physiological processes,
53 including development, growth polarity or movement, the internal clock(s) and interaction with the
54 biotic and abiotic environment. Naturally occurring photoreceptors typically consist of a prosthetic
55 chromophore and an apoprotein, responsible for light perception and signal transduction respectively.
56 This generic description applies to most of the photoreceptors found in plants, including tetrapyrrole-
57 binding phytochromes, flavin-based cryptochromes and receptors that contain Light–Oxygen–Voltage
58 (LOV) motifs and retinal-associated rhodopsins (Sineshchekov, Jung and Spudich, 2002; Paik and Huq,
59 2019). An exception is instead represented by UVR8 and homologs, whose UV light sensing ability is
60 intrinsic to the protein, by virtue of two to four tryptophan residues (Tilbrook *et al.*, 2013). Each
61 photoreceptor perceives to a specific range of visible light spectrum, with some overlaps. Their
62 sensitivity concentrates over red and blue wavelengths, which are especially relevant for
63 photosynthesis, and high-energy, thus potentially harmful, light. In response to these stimuli, higher
64 plant photoreceptors control flavonoid and chlorophyll biosynthesis, clock entrainment, phototropism,
65 reproductive development (flowering and tuberization), stomatal opening and chloroplast movement
66 (Möglich *et al.*, 2010).

67 To the repertoire of naturally-occurring photoreceptors, synthetic biologists have added new ones,
68 exploiting the possibility of domain shuffling across organisms. This has expanded the possibility to fine-
69 tune molecular processes in response to specific light stimuli. Several plant photoreceptors and their
70 protein partners have been deployed to harness light-elicited processes in animal cells, for example
71 through engineering Arabidopsis FKF1 (Yazawa *et al.*, 2009), cryptochromes, UVR8 (Kennedy *et al.*,
72 2010) and phytochromes (Müller *et al.*, 2013). On the other hand, plant optogenetics has lagged behind,
73 due to the extant overlap with a plethora of endogenous photoreceptors. Pioneering efforts in this
74 direction include protein mutagenesis aimed at producing slow-photocycling phototropin variants (Hart
75 *et al.*, 2019), or engineering green-light perception through synthetic transcriptional regulators inspired
76 to prokaryotic systems (Chatelle *et al.*, 2018). Main approaches to the engineering of synthetic genetic
77 switches in plant have been recently reviewed (Andres, Blomeier and Zurbriggen, 2019).

78 Few studies so far sought to engineer new layers of regulation in plant organelles, such as mitochondria
79 and chloroplasts, through synthetic biology approaches, to improve the efficiency of cellular energy
80 factories (Nielsen *et al.*, 2013; Xiang *et al.*, 2020), or to introduce novel methods of transcriptional

81 regulation (Verhounig, Karcher and Bock, 2010). Here we propose the implementation of a new
82 chloroplast-localized synthetic photoswitch, based on a photoreceptor-associated protein-fragment
83 complementation assay (PCA). PCAs exploit the affinity between two peptides fused to split-protein
84 fragments that, when brought in close proximity, reconstitute the activity of the original protein
85 (Merezhko *et al.*, 2020; Wang *et al.*, 2020).

86 Our photoswitch system is based on cyanobacterial Orange Carotenoid binding Proteins (OCPs) (Kay Holt
87 and Krogmann, 1981; Kerfeld *et al.*, 2003), which, when activated by blue-green light, undergo
88 reversible conformational changes that enable phycobilisome photoprotection (Wilson *et al.*, 2006,
89 2008; Kirilovsky and Kerfeld, 2013). OCPs are water-soluble proteins, whose structure is mainly
90 composed of a C-terminal domain (CTD) and an N-terminal domain (NTD) connected by a flexible linker
91 (Wu and Krogmann, 1997; Kerfeld *et al.*, 2003). The OCP apoprotein non-covalently incorporates a single
92 keto-carotenoid molecule, such as canthaxanthin, 3'-hydroxyl-echinenone or echinenone, as prosthetic
93 group buried inside the two domains (Punginelli *et al.*, 2009). OCP photoactivation is accompanied by
94 extensive reconfiguration of carotenoid-protein interactions, with the consequent translocation of the
95 pigment within the protein (Gupta *et al.*, 2015; Leverenz *et al.*, 2015; Bondanza *et al.*, 2020).
96 Photoconversion is possible only when a keto-carotenoid is buried inside the protein, whilst association
97 with other carotenoids inhibits its photoconversion ability (Punginelli *et al.*, 2009; Wilson *et al.*, 2011).

98 Here, we report the genetic engineering of *Arabidopsis thaliana* plants to express the chimeric
99 photoswitch based on OCPs and the NanoLuc luciferase protein, together with a bacterial enzyme for
100 keto-carotenoid biosynthesis to generate the necessary prosthetic group (Ruiz-Sola and Rodríguez-
101 Concepción, 2012; Nisar *et al.*, 2015; Bai *et al.*, 2017). We also describe the application of transient
102 transformation systems to fully characterise the dynamics of such synthetic construct to establish the
103 bases of its future applications.

104

105

106 RESULTS

107 Design of a photo-switchable device based on OCP properties

108 To engineer a light-dependent molecular switch to be orthogonally active in plant plastids, we focused
109 on the class of the cyanobacterial Orange Carotenoid-binding Proteins (OCPs). Among the three known
110 paralogous families of OCPs (OCP, OCP2 and OCPX), we reckoned the OCP2 family to fit better the
111 rational design of a synthetic photoreceptor. Indeed, its faster conversion kinetics, its monomeric state,
112 and its ability to revert to the dark-adapted state (OCP2⁰) in the absence of a helper protein (Bao *et al.*,
113 2017) reduce the number of components required for the photoswitch to function. Thus, we selected
114 the OCP2 coding sequence (CDS) from the cyanobacterium *Fischerella thermalis* and separated its N-
115 terminal domain (NTD, 165 aa) and C-terminal domain (CTD, 131 aa). *F. thermalis* was chosen as the
116 source organism as one of the few known to encode for an OCP2 protein as the sole OCP sequence in its
117 genome (Bao *et al.*, 2017). Moreover, being *F. thermalis* a thermophilic organisms (Alcorta *et al.*, 2019),
118 proteins encoded by its genome likely have higher stability compared to the case of non-thermophilic
119 ones. To test whether these modules reconstitute a complex capable of light-dependent regulation in
120 angiosperm cells, we generated a synthetic construct that couples a luminescent output with
121 dimerisation (Fig. 1). In our design, we exploited the affinity and light-driven separation of the two OCP2
122 modules for a protein complementation assay, based on a NanoLuc complementation assay developed
123 in mammalian cells and called NanoBit (Dixon *et al.* 2016).

124 We fused each domain with one of the two fragments of the split-NanoLuc protein: the N-terminal
125 (NNLuc, 159 aa) and the C-terminal (CNLuc, 11 aa) fragments. In this way, we generated two chimeric
126 constructs which, together, constitute a split-NLucOCP2 photoswitch. In the wild-type OCP2 protein, the
127 two domains associate by means of a flexible linker and by the non-covalent bonds that a single keto-
128 carotenoid molecule establishes after its incorporation inside the OCP2 protein (Wu and Krogmann,
129 1997; Kerfeld *et al.*, 2003) (Fig. 1A-B). Instead, in our synthetic construct, the OCP2 modules are kept
130 together exclusively by their interactions with the keto-carotenoid (Fig. 1B). Since the strength of these
131 interactions depends on the light-dependent translocation of the keto-carotenoid inside the OCP2
132 structure (Gupta *et al.*, 2015; Leverenz *et al.*, 2015; Bondanza *et al.*, 2020), we expected the NTD and the
133 CTD to associate in the dark, whereas exposure to blue-green light would bring them apart.

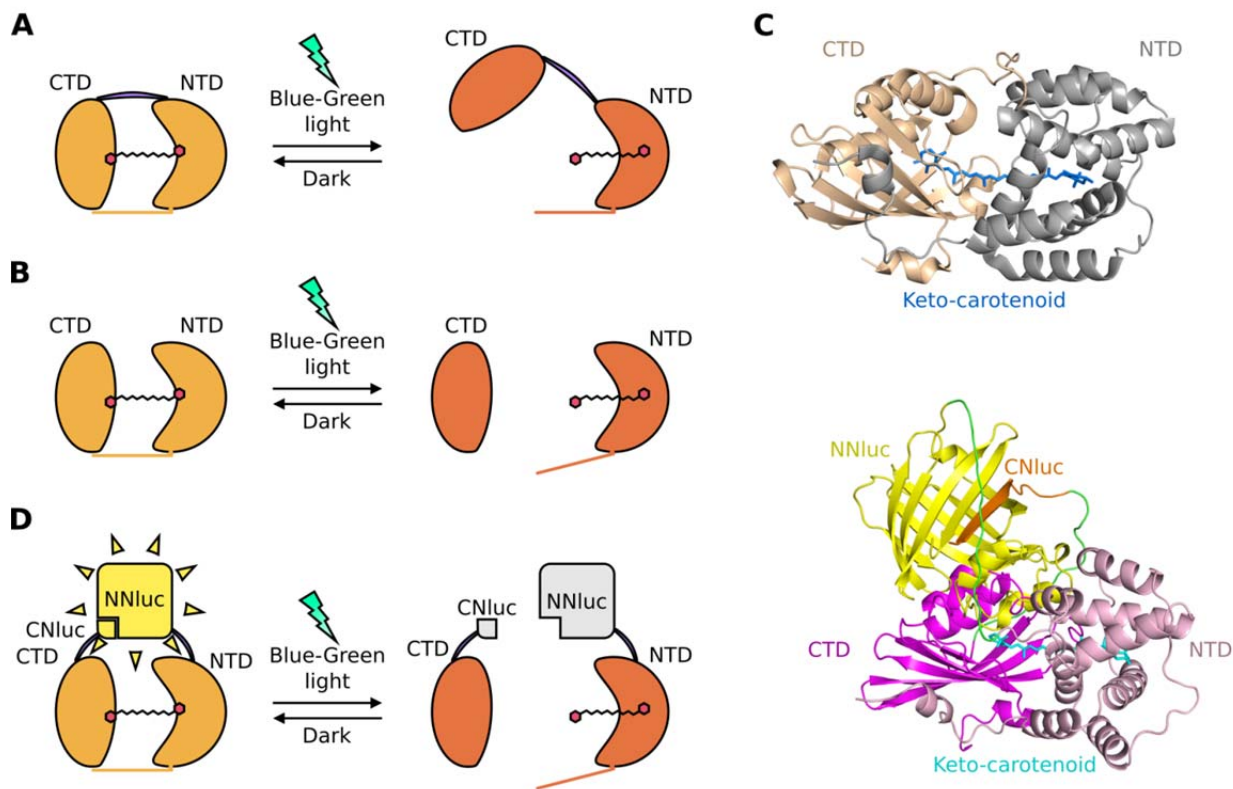
134 Specifically, we fused the NNLuc to the C-terminus of the NTD module (NTD-NNLuc), and the CNLuc to the
135 N-terminus of the CTD module (CNLuc-CTD). This conformation was selected following an *in silico*
136 prediction based on the 3D structures of NanoLuc (Protein Data Bank (PDB) ID 5IBO) and the OCP from
137 *Limnospira maxima* (PDB ID 5UI2), which shares the strongest sequence similarity with FtOCP2 among

138 the OCPs whose structure has been experimentally determined. This model suggested these fusions as
139 the best option to bring the NanoLuc modules in close proximity in the closed (OCP⁰) conformation (Fig.
140 1C).

141 We predicted that the interaction between the NTD and the CTD in the dark would reconstitute the
142 enzymatic NanoLuc activity and therefore produce a luminescent output upon addition of the
143 furimazine substrate to plant cell extracts (Hall *et al.*, 2012; Dixon *et al.*, 2016). On the other hand, we
144 expected blue-green light exposure to promote detachment of the CTD from the NTD, resulting in the
145 disruption of the NanoLuc complementation (Fig. 1D). The low affinity between the NNLuc and the CNLuc
146 themselves (Dixon *et al.* 2016), allowed us to rule out that the reconstitution of the NanoLuc activity
147 would only be due to their interaction.

148

149



150

151

152 **Figure 1.** Rational design of a blue-green photoswitch based on OCP2 modules and the NanoLuc complementation
153 system (split-NLucOCP2).

154 A, Scheme of the light-induced native OCP2 protein dynamics: dark state (left), called OCP2 orange (OCP2^O), and
155 light-induced state (right), known as OCP2 red (OCP2^R). B, N-Terminal Domain (NTD) and C-Terminal Domain (CTD)
156 interactions, when expressed as separate peptides, in darkness (left) or under stimulating light. C, *In silico*
157 prediction of dark OCP2 (top) and dark split-NlucOCP2 (bottom) 3D structures. D, Scheme of the split-NlucOCP2
158 photoswitch. In the dark, the two OCP2 modules interact with each other, thus bringing the two NanoLuc
159 fragments in close proximity and complementing NanoLuc; blue-green light leads to a separation of the two
160 modules, suppressing NanoLuc activity.

161

162 **Generation and characterization of canthaxanthin-producing Arabidopsis transgenic plants**

163 Both the interaction and the photoconversion of the OCP2 modules depend on the presence of specific
164 keto-carotenoids (canthaxanthin, 3'-hydroxyl-echinenone or echinenone) (Punginelli *et al.*, 2009). For
165 our synthetic photoswitch to be functional, one of the two modules, usually the NTD (Lechno-Yossef *et al.*
166 *et al.*, 2017), should be conjugated with a single molecule of the proper keto-carotenoid. Therefore, we
167 generated stable transgenic Arabidopsis lines expressing the β -carotene ketolase (*crtW*) enzyme from
168 *Agrobacterium aurantiacum*, which catalyzes canthaxanthin biosynthesis from β -carotene (Fig. 2A) via
169 the addition of a carbonyl group to carbon 4 and 4' of the substrate (Misawa *et al.*, 1995; Choi *et al.*,
170 2005; Bai *et al.*, 2017). It is important to note that the *crtW* enzyme is also involved in the biosynthetic
171 pathway of another ketocarotenoid, astaxanthin, by using zeaxanthin as substrate. Moreover,
172 canthaxanthin itself can be hydroxylated by an endogenous β -hydroxylase enzyme, leading to
173 astaxanthin production (Zhong *et al.*, 2011). Since carotenoid biosynthesis in higher plants occurs in
174 plastids (Nisar *et al.*, 2015), we fused the sequence of the *crtW* enzyme with a previously tested plastid
175 localization sequence (PLS) from ribulose 1,5 bisphosphate carboxylase of *Pisum sativum* (Fig. 2B), and
176 placed this *PLS-crtW* transgene under the control of the constitutive *Cauliflower mosaic virus* (CaMV)
177 35S promoter.

178 Following positive selection on kanamycin, 21 putative transformants were isolated. To evaluate the
179 actual expression of the transgene, we measured the *PLS-crtW* transcript level through real time
180 quantitative PCR (RT-qPCR) and correlated it to the content of ketocarotenoids, as measured by High
181 Performance Liquid Chromatography (HPLC) (Fig. 2C). All selected *35S:PLS-crtW* plants actively
182 expressed the transgene with extensive variability. Out of 13 lines analysed, 10 expressed detectable
183 levels of keto-carotenoids, ranging from 4% to 21% of the total pigment content (Fig. 2C). Astaxanthin
184 was the most abundant keto carotenoid accumulated, but all 10 lines also contained the OCP-binding
185 canthaxanthin. Keto carotenoids were synthesized at the expense of the β - β xanthophyll neoxanthin and
186 violaxanthin, which were reduced with respect to the parental lines. Zeaxanthin was not detected in any

187 plant in the light regime used in this analysis. Total carotenoid content was not different between the
188 genotypes.

189

190 **Table 1.** Comparison of the carotenoid content in *crtW* and wild-type *Arabidopsis* plants. Data are percentages of
191 each pigment relative to the total carotenoid content per each line. Average and standard deviation are shown per
192 each group of lines. A Student T-test was used to assess significant differences between *crtW* and Col-0 genotypes.
193 Different letters between rows represent differences in carotenoid content ($p < 0.05$).

194

Genotype	Neoxanthin	Violaxanthin	Lutein	β -carotene	Astaxanthin	Canthaxanthin
<i>crtW2</i>	15.62	10.83	56.03	12.90	3.52	1.83
<i>crtW3</i>	10.55	4.22	56.34	14.76	10.89	3.24
<i>crtW9</i>	12.15	6.34	56.51	12.99	9.56	2.45
<i>crtW11</i>	9.36	4.88	54.34	10.17	15.41	5.84
<i>crtW12</i>	14.45	9.97	54.78	14.04	5.30	1.45
<i>crtW13</i>	1.73	11.99	57.89	11.00	12.97	4.42
<i>crtW14</i>	9.12	6.12	50.17	19.39	10.84	4.35
<i>crtW17</i>	9.77	4.33	48.50	18.35	15.80	3.25
<i>crtW19</i>	13.89	7.27	51.47	17.33	5.91	4.12
<i>crtW20</i>	10.42	7.15	49.54	20.93	9.03	2.93
	10.71 \pm 3.89 ^a	7.31 \pm 2.75 ^a	53.56 \pm 3.35 ^a	15.19 \pm 3.64 ^a	9.92 \pm 4.15	3.39 \pm 1.33
<i>crtW10</i>	15.07	13.32	57.54	14.06	0	0
<i>crtW16</i>	13.90	10.94	54.44	20.72	0	0
<i>crtW18</i>	15.14	13.23	55.62	16.01	0	0
	14.70 \pm 0.7 ^a	12.50 \pm 1.35 ^b	55.87 \pm 1.57 ^a	16.93 \pm 3.42 ^a	0	0
Col-0	11.94	11.69	52.37	24.00	0	0
Col-0	15.02	12.07	55.96	16.95	0	0
	13.48 \pm 2.18 ^a	11.88 \pm 0.27 ^b	54.17 \pm 2.54 ^a	20.47 \pm 4.99 ^a	0	0

195

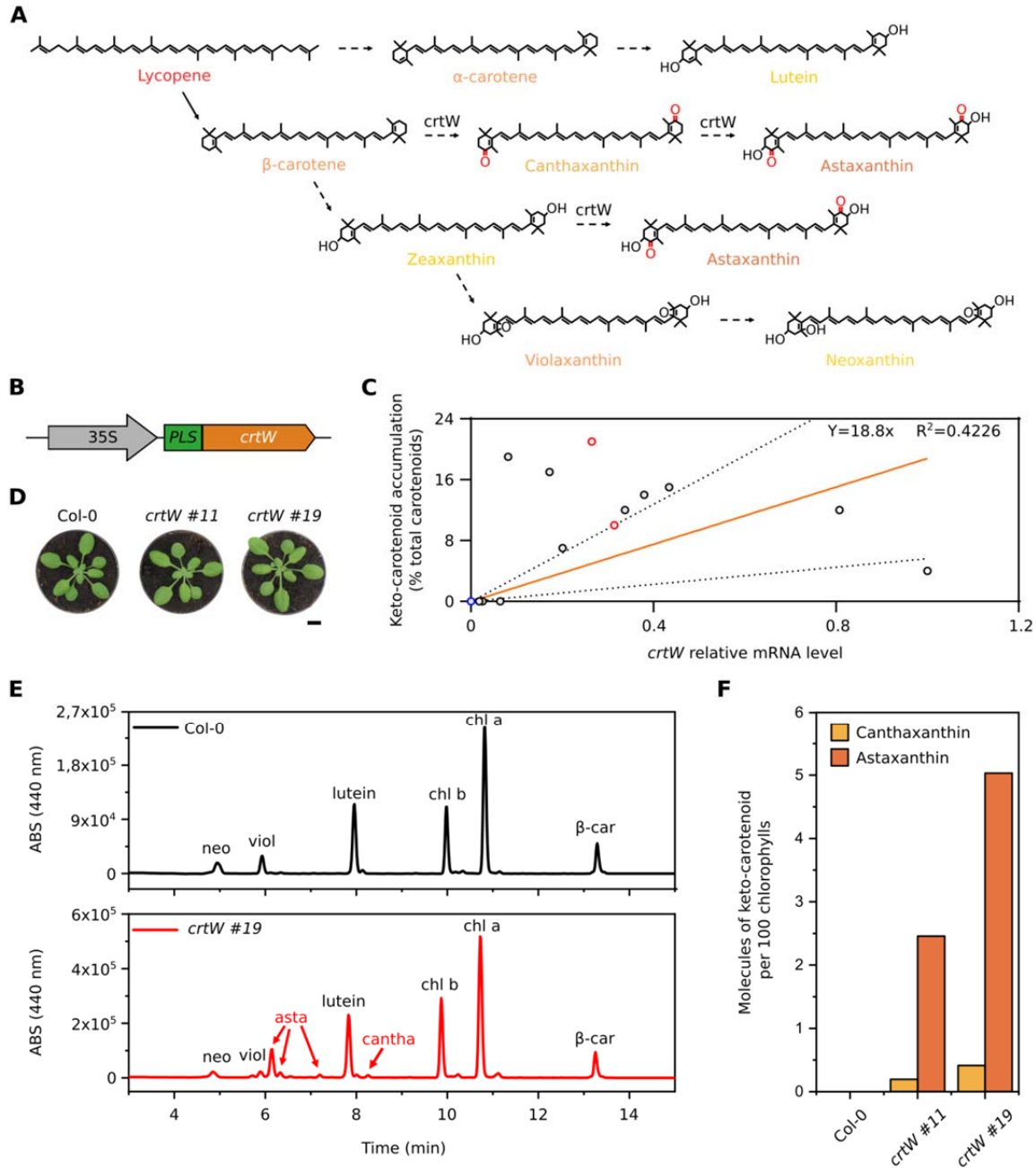
196 Two independent lines with high and intermediate keto-carotenoids content (Fig. 2C, red circles, and
197 Fig. 2D) were further analyzed (Fig. 2E and Fig. 2F). At a visual inspection, the two transgenic lines
198 showed a slightly brown pigmentation compared to the wild-type, which was only partially confirmed by
199 a phenotyping analysis based on RGB imaging of the plants through a commercial phenotyping machine.
200 Comparing Col-0, *crtW #11* and *crtW #19* genotypes at 17, 21 and 24 days after germination, we found
201 no significant difference in the average size of the plants, and comparison of the three components of
202 the RGB images (Red, Green and Blue) showed a statistically significant increase in the red component
203 between the 17 and 21 days old Col-0 and *crtW #19* (Supplemental Fig. S1). Considering the gathered

204 evidence collectively, we concluded that the implementation of the endogenous carotenoid biosynthetic
205 pathway allowed the production of keto-carotenoids in Arabidopsis.

206

207

208



209
210

211 **Figure 2.** Pigment content analysis of keto-carotenoid *Arabidopsis thaliana* transgenic lines.
212 A, Overview of the biosynthetic carotenoid pathway after the addition of the *crtW* enzyme; dotted arrows
213 represent multiple enzymatic steps. B, Scheme of the synthetic construct for canthaxanthin production:
214 *Cauliflower mosaic virus* 35s promoter (CaMV35s); Plastid localization sequence (PLS); β -carotene ketolase (*crtW*).
215 C, Relative *crtW* mRNA levels and their corresponding keto-carotenoid content in 13 independent transgenic lines
216 (black and red circles) and one Col-0 (blue circle); red circles represent the two lines (#11 and #19) chosen for the
217 following experiments. mRNA levels in the graph are relative to the transgenic line with the highest expression, set
218 as 1. The orange line represents the curve fitted to the data with linear regression, and the dotted lines are the
219 95% prediction confidence intervals. The R squared (R^2) and the equation of the curve are shown. D, Phenotypic
220 comparison between *Arabidopsis* Col-0 plants and two independent *crtW* transgenic lines. E, HPLC analysis for
221 canthaxanthin and astaxanthin detection in a *crtW* line (red line), compared with a Col-0 plant (black line);
222 neoxanthin (neo), violaxanthin (viol), astaxanthin (asta), canthaxanthin (cantha), chlorophyll b (chl b), chlorophyll a
223 (chl a), β -carotene (β -car). F, Quantitative measurement of canthaxanthin and astaxanthin, represented as
224 molecules of keto-carotenoid per 100 molecules of chlorophylls.

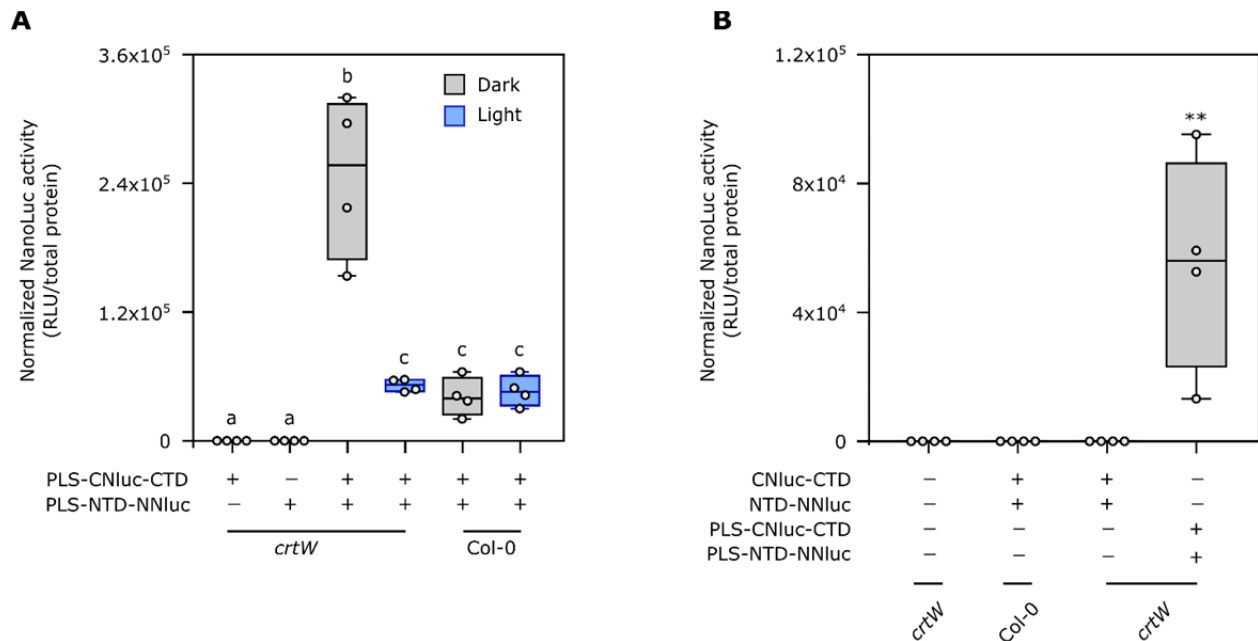
225
226

227 **Testing of OCP2-based photoswitch in plant protoplasts**

228 We generated plasmids carrying the NTD-NNLuc and CNLuc-CTD transgenes, each equipped with a plastid
229 localization signal (PLS), to be expressed under control of the 35S CaMV promoter, and we tested the
230 functionality of the photoswitch system in transient assays in mesophyll protoplasts. We started by
231 investigating the activity of the constructs in protoplasts isolated from either Col-0 or *crtW* plants, to
232 assess whether keto-carotenoids were required for the output of the system, according to our rational
233 design.

234 A first proof-of-principle experiment was performed to evaluate the responsivity of the system to the
235 blue-green light stimulus and its basal activity. All possible combinations (Fig. 3A) of the two modules
236 were transformed in *crtW* protoplasts. Sixteen hours after the transformation, dark-incubated
237 protoplasts were treated under blue-light (465-480 nm, $350 \mu\text{mol m}^{-2} \text{s}^{-1}$) for 1 hour, while control
238 samples were maintained in the dark. Protoplasts transformed with PLS-CNLuc-CTD or PLS-NTD-NNLuc
239 alone showed no luminescent output in the dark, confirming that the two NanoLuc fragments did not
240 retain any basal enzyme activity (Fig. 3A). Those transformed with both modules were instead analysed
241 for light response. High luminescence output in dark-treated protoplast was suggestive of effective
242 complementation and reconstitution of a dark-adapted state in the OCP2 complex. The output was
243 instead significantly lower in illuminated protoplasts, indicating the detachment of the OCP2 modules,

244 as expected, with consequent disruption of the enzymatic activity (Fig. 3A). Wild-type protoplasts had
 245 identical output upon dark or light treatment, suggesting that light is unable to trigger the structural
 246 changes in the OCP2 complex in the absence of the proper keto-carotenoids. The residual activity
 247 recorded in the wild-type background pointed at the occurrence of some extent of unspecific interaction
 248 between the two photoswitch modules, likely due to the affinity of the OCP2 fragments. Remarkably,
 249 however, blue-green light treatment in the *crtW* background cut the output down to the level
 250 associated with unspecific module interaction (Fig. 3A), suggesting that the keto-carotenoid dependent
 251 changes that are typical of the native OCP2 protein were fully recapitulated in our split configuration.
 252 Next, we investigated the effect of a different subcellular localization of the photoswitch modules. In
 253 plants, carotenoids are mainly concentrated inside plastids, and no specific or generic carotenoid export
 254 system is known (Sun *et al.*, 2018). To exclude our photoswitch from plastids, we generated two new
 255 versions of the CNluc-CTD and NTD-NNluc modules devoid of PLS. The new modules were again tested
 256 both in *crtW* and Col-0 protoplasts, using the plastid localized photoswitch as positive control for the
 257 NanoLuc activity. We found that the luminescent signal produced in the cytosol-localized photoswitch
 258 modules was comparable to that of untransformed protoplasts (Fig. 3B), confirming that our
 259 photoswitch can only be active in carotenoid-containing organelles.
 260



261

262

263

Figure 3. Activity of the synthetic photoswitch in a transient protoplasts assay.

264 A, Light response in Arabidopsis Col-0 and transgenic *crtW* -isolated protoplasts. Different letters indicate
265 statistical differences ($P \leq 0.05$) calculated from one-way ANOVA ($n=4$) followed by Tukey's post-hoc test. "Light"
266 indicates treatment under blue-green light ($465\text{-}480\text{ nm}$, $350\text{ }\mu\text{mol }\mu\text{m}^{-2}\text{ s}^{-1}$) for 1 h. B, Comparison between
267 plastidial and non-plastidial localization of photoswitch components. Protoplasts were treated with either dark or
268 blue light ($350\text{ }\mu\text{mol }\mu\text{m}^{-2}\text{ s}^{-1}$) for 1 hour. Asterisks indicate statistical differences ($P \leq 0.01$, $n=4$). In the box plots,
269 dots represent single data points, the black line marks the median, and the box indicates the interquartile range
270 (IQR). Whiskers extend to data points below $1.5 \times$ IQR away from the box extremities.

271

272 **Characterization of split-NlucOCP2 light-responsiveness and reversion**

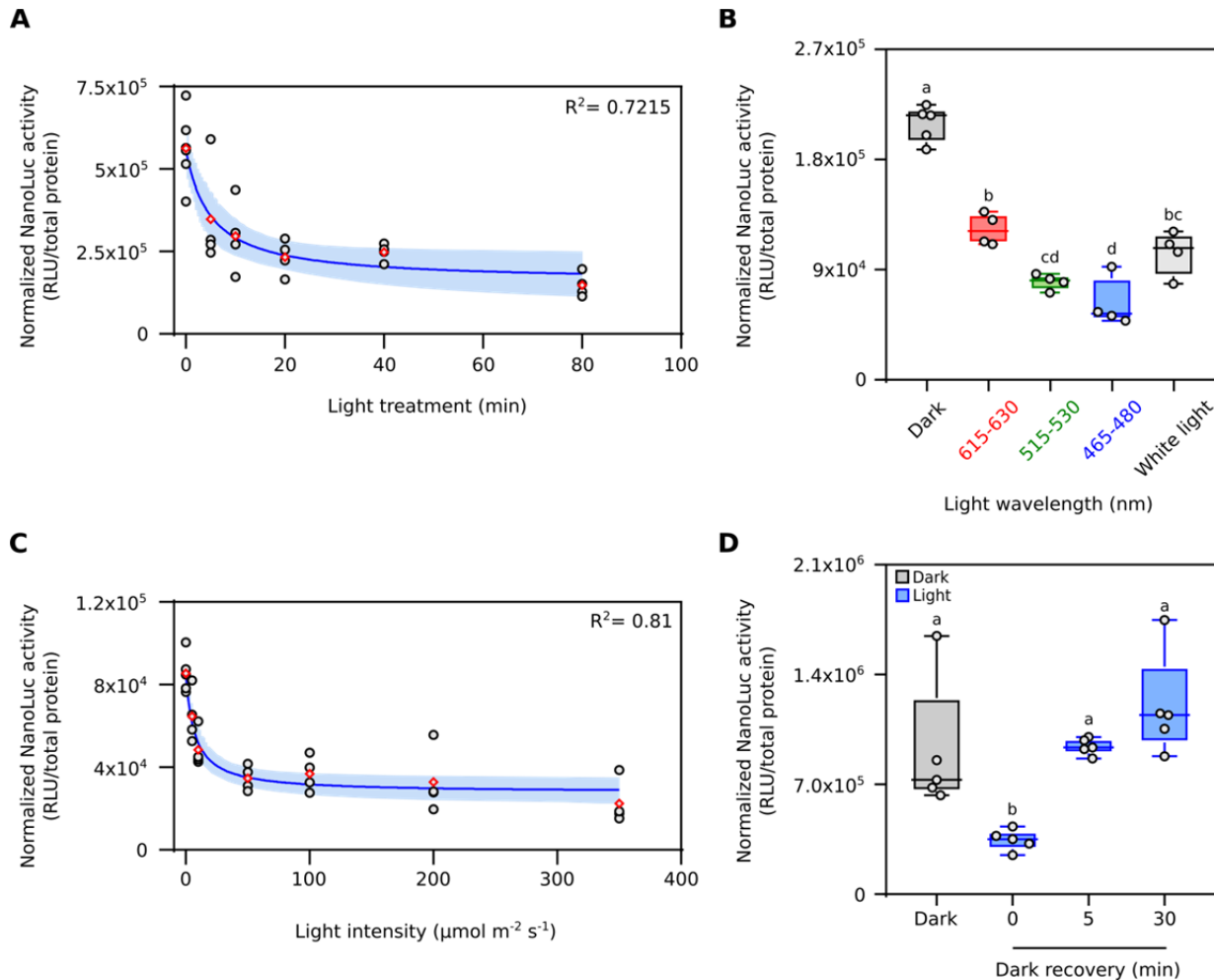
273

274 Once we found out the basal requirements of our photoswitch, we performed a full characterization of
275 its dynamics, to describe how its activity could be modulated by the light. First, to understand the kinetic
276 of the light-induced structural changes in the photoswitch, we treated the transformed *crtW* protoplasts
277 for different periods with white light ($350\text{ }\mu\text{mol m}^{-2}\text{ s}^{-1}$), from 5 to 80 minutes, after dark incubation.
278 Photoconversion of a significantly high amount of the complex occurred as early as 5 mins after light
279 exposure and increased further with time (Fig. 4A). We selected 20 mins light treatment for further
280 analysis, since this data point was associated with a low variability among the biological replicates. Next,
281 we investigated whether light quality is relevant for the regulation of our photoswitch activity, and
282 which wavelength range is the most effective in triggering the switch. Treatments with a tuneable led
283 lamp emitting red ($615\text{-}630\text{ nm}$), green ($515\text{-}530\text{ nm}$), blue ($465\text{-}480\text{ nm}$) or white light were compared
284 with dark treated samples (Fig. 4B). We observed that the output was significantly different between the
285 dark treatment and the whole set of different wavelengths: blue and green light exerted the strongest
286 effect, while red light only halved the luminescent output. White light was not as effective as blue light
287 to switch off the system, suggesting that saturated blue light is required to achieve the maximum
288 photoswitch performance.

289 Having established the optimal treatment duration (20 minutes) and light spectrum (blue) to elicit
290 photoswitch output, we moved on to analyse the effect of light intensity on our system, testing the
291 range from 5 to $350\text{ }\mu\text{mol m}^{-2}\text{ s}^{-1}$ (Fig. 4C). We could measure significant signal decrease already at $10\text{ }\mu\text{mol m}^{-2}\text{ s}^{-1}$.
292 The response was saturated at $50\text{ }\mu\text{mol m}^{-2}\text{ s}^{-1}$. Finally, we investigated the possibility that
293 our synthetic photoswitch could revert from the dissociated to the dimeric form when light exposure
294 ceases, as happens for heterodimeric OCP2 complexes *in vitro* (Lechno-Yossef *et al.*, 2017). We shifted
295 protoplast samples, previously exposed to 20 min saturating blue light ($50\text{ }\mu\text{mol m}^{-2}\text{ s}^{-1}$), to darkness for
296 different amounts of time. We found out that the split-NlucOCP2 had the capacity to revert quickly to

297 the dark-adapted conformation after the treatment, since we measured full recovery of the signal as
 298 early as 5 min into dark incubation (Fig. 4D).

299
 300



301
 302 **Figure 4.** Characterization of the split-NlucOCP2 photoswitch in *Arabidopsis thaliana* protoplasts.
 303 A, Impact of different lengths of light exposure (white light, $350 \mu\text{mol m}^{-2} \text{s}^{-1}$) on photoswitch output. Data points
 304 correspond to 0, 5, 10, 20, 40 and 80 minutes. B, Effect of different wavelengths on the output of the photoswitch,
 305 as compared to darkness. Red, green, blue or white light was supplied for 20 minutes at $350 \mu\text{mol m}^{-2} \text{s}^{-1}$. C,
 306 Output modulation under increasing light intensity. Protoplasts were exposed to 5, 10, 50, 100, 200, or $350 \mu\text{mol}$
 307 $\text{m}^{-2} \text{s}^{-1}$ blue light for 20 minutes after 16 h dark incubation (initial data point). D, Test of the reversibility of the
 308 photoswitch. After light treatment (20 minutes, $50 \mu\text{mol m}^{-2} \text{s}^{-1}$, blue light), the samples were incubated for 5 or 30
 309 min in the dark before sampling. In the box plots, dots represent single data points, the black line marks the
 310 median, and the box indicates the interquartile range (IQR). Whiskers extend to data points that are below 1.5 X
 311 IQR away from the box extremities. Different letters indicate statistical differences ($P \leq 0.05$) calculated from one-

312 way ANOVA followed by Tukey's post-hoc test. In dot plots, data fitting through non-linear regression analysis is
313 shown with blue continuous curves, generated using the GraphPad Prism built-in equation for [Inhibitor] vs.
314 response model. Shaded bands indicate the predicted 95% confidence interval. Black dots represent single data
315 points and red rhombuses represent mean values. The R squared (R^2) of the curves are included in the graphs.

316

317

318 DISCUSSION

319 In this work, we successfully exploited the properties of a cyanobacterial Orange Carotenoid Protein to
320 generate a synthetic photoswitch meant to be active in plant chloroplasts (Fig. 3B). We were able to
321 draw a complete characterization of the prototype version of our synthetic photoswitch, split-NlucOCP2,
322 in living plant cells, thanks to a strategy based on protoplast transformation. Synthetic biology
323 endeavours in plants are complicated by non-negligible hurdles associated with genetic engineering,
324 such as long timeframes for the generation of transgenic individuals, low rates of homologous
325 recombination and, in some cases, cumbersome procedures for plant genetic transformation. However,
326 populations of isolated cells, obtained from the enzymatic digestion of cell walls from plant tissues
327 (typically young, poorly lignified leaves), can be adopted as an easy and convenient alternative to
328 implement fast, combinatorial and high-throughput tests for newly designed synthetic devices (Yoo, Cho
329 and Sheen, 2007; Pouvreau *et al.*, 2020). We therefore opted for this strategy to characterize the
330 modules of split-NlucOCP2.

331 As according to our design (Fig. 1D), this system was inhibited by light inputs; the stimulus was sufficient
332 to promote the maximum extent of monomerization of the system, indicated by the activity observed in
333 the Col-0 background (Fig. 3A). Another important feature of the photoswitch was its ability to revert
334 spontaneously to the heterodimeric (dark-adapted) state after the light-induced monomerization (Fig.
335 4D). The extent of output inhibition by light was directly proportional to the treatment duration and
336 intensity (Fig. 4A and C). Altogether, this evidence let us conclude that split OCP2 strategies are viable to
337 design fast-responding and quickly reversible photoswitches, characterized by a continuous response to
338 light and a high dynamic range. The blue and green ranges of the light spectrum were the most effective
339 ones in switching off the response (Fig. 4B). Since white light contains blue, green and red wavelengths,
340 we were not surprised by its effect on the switch (Fig. 4B); the ability of red light to inactivate our
341 photoswitch, however, was unexpected, since OCP2 has an absorption peak in the blue-green range at
342 474 and 502 nm and cannot be photoactivated by red-light (Bao *et al.*, 2017). We may speculate that
343 this effect is caused by differences in the spectral properties of both the keto-carotenoid, due to the
344 protein environment, and the protein, since we are expressing a split and engineered version of it.

345 Two features proved to be essential for the synthetic photoswitch to control luciferase activity: firstly,
346 chloroplasts needed to produce the required keto-carotenoid prosthetic group and, secondly, the two
347 photoswitch modules required plastidial localization. Thus, we had to implement a canthaxanthin
348 biosynthetic pathway by expressing an exogenous β -carotene ketolase (*crtW*) enzyme, which catalyzes

349 canthaxanthin biosynthesis (Fig. 2). Indeed, when protoplasts expressed cytosol-localized modules (Fig.
350 3A) or were unable to produce keto-carotenoids (Fig. 3B), the switch was non-functional. Dimerization
351 and photoactivation of the photoswitch could be related to either canthaxanthin or astaxanthin, which
352 in both cases were recently demonstrated to be bound by OCP2, in the case of heterologous expression
353 of this subunit in the green alga *Chlamydomonas reinhardtii* engineered for producing keto-carotenoids
354 (Pivato et al resubmitted). In the keto-carotenoid producing plants, we found that astaxanthin was
355 reproducibly more abundant than canthaxanthin (Fig. 2F and Table 1). This is not entirely
356 unexpected/surprising, given previous demonstrations that the addition of the *crtW* enzyme in plant
357 provides only one pathway towards canthaxanthin, whereas more pathways converge towards
358 astaxanthin production (Bai *et al.*, 2017), one of which using canthaxanthin as a substrate. Comparison
359 of the composition of the carotenoid pool in *crtW* and wild-type plants showed that keto-carotenoids
360 were synthesized at the expense of other β - β xanthophylls. As shown in Table 1, neoxanthin, β -carotene
361 and violaxanthin present lower average values in keto-carotenoids producing lines, even though only
362 the latter shows a statistical significance. This was expected, because β -carotene and zeaxanthin are
363 substrate of the *crtW* enzyme, but also precursors of both neoxanthin and violaxanthin (Fig. 2A). On the
364 other hand, ϵ - β xanthophyll lutein, whose biosynthesis follows a different branch of the pathway, (Ruiz-
365 Sola and Rodríguez-Concepción, 2012; Bai *et al.*, 2017) was unaffected (Fig. 2A).

366 Light exposure could not abolish OCP2-nanoLuc signal entirely, even after several hours. The signal still
367 present in light-treated *crtW* protoplasts (Fig. 3A) can be explained by two non-mutually exclusive
368 hypotheses: that the treatment could not separate the whole pool of interacting NTD-CTD modules, or
369 that other carotenoids, such as β -carotene, may mediate modules interaction, although without the
370 ability to photoconvert (Punginelli *et al.*, 2009; Wilson *et al.*, 2011). Recently, *Fischerella thermalis* OCP2
371 was shown to bind neoxanthin, lorenzoanthin and lutein when heterologously expressed in
372 *Chlamydomonas reinhardtii* (Pivato et al. resubmitted). The latter scenario could also explain the
373 amount of signal we measured in dark treated wild-type protoplasts, which was not affected by the light
374 treatment (Fig. 3A). Moreover, the complete absence of signal observed in the cytosol-localized
375 photoswitch suggests that none of the carotenoids able to conjugate with OCP2 were present outside
376 the chloroplast in sufficient amounts to associate with the photoswitch (Fig. 3B).

377 The success of this initial study lays the foundations for different ways in which our system could be
378 exploited in the future. Similar to NanoLuc, the OCP2 modules can be fused to a bipartite enzyme or
379 structural protein whose function is favoured under dark conditions and/or not required or even

380 detrimental when cells are illuminated. Alternatively, the OCP2 modules could serve for reversible
381 association of an inhibitor protein, thus leading to positive regulation upon light exposure and
382 repression in darkness. While potentially presenting a limitation for use in plants that are not able to
383 synthesize keto-carotenoids, our system could be exploited not only for its photo-induced activity, but
384 also as a carotenoids biosensor: when carotenoids (β -carotene, zeaxanthin) are present in the cellular
385 environment, a small percentage of the modules is expected to dimerize in a stable manner; instead, if
386 in case of canthaxanthin, 3'-hydroxyl-echinenone or echinenone accumulation, the dimerization rate will
387 be higher and reversible under light treatment (Fig. 3A). Alternatively, this photoswitch strategy might
388 be applied in microalgae, where different species accumulate keto-carotenoids or can be successfully
389 engineered to express them (Perozeni *et al.*, 2020).

390 In summary, here, we demonstrated that plant organelles can be equipped with an orthogonal synthetic
391 photoswitch, based on a cyanobacterial light-responsive protein and its cognate keto-carotenoids. The
392 behavior of this synthetic construct led us to conclude that, the structural modularity of OCP, together
393 with its light-driven dissociation (Leverenz *et al.*, 2014; Lechno-Yossef *et al.*, 2017), makes it a suitable
394 tool for optogenetic applications (Dominguez-Martin and Kerfeld, 2019). Selecting biological modules
395 from unrelated species grants the highest probability that cross-interactions between components and
396 endogenous pathways are kept to a minimum, and we consider particularly interesting the ability of
397 OCPs to be triggered by the green range of the light spectrum, considering that it should not interfere
398 and stimulate the most common photoreceptors already known inside the plant systems, ensuring the
399 orthogonality of the system. We believe that this pioneer study establishes the basis for future
400 implementation of plastid optogenetics to regulate organelle responses, such as gene transcription or
401 enzymatic activity, upon exposure to specific light spectra.

402

403 **MATERIALS AND METHODS**

404 **Design of synthetic DNA sequences and plasmid assembly**

405 Sequences were designed, codon-optimized for *A. thaliana* expression and synthesized as DNA strings
406 using the GeneArt service (Thermo-Fisher Scientific). The sequences of the synthetic constructs devised
407 for this work is provided in Supplemental Information S1. Directional cloning of DNA fragments was
408 performed using the pENTR™ Directional TOPO® Cloning Kits (Thermo-Fisher Scientific). For the OCP2
409 modules we took the *Fischerella thermalis* OCP2 sequence as reference (accession WP_009459388). The

410 non-chloroplast localized fragments were amplified with the Phusion™ High-fidelity DNA polymerase
411 (Thermo-Fisher Scientific) using the following primer couples: NTD-NNluc-Fw
412 (CACCATGTCCTTCACCATCGAG) with NTD-NNluc-Rv (TCAGCTGTTGATGGTCACTCTG) and CNluc-CTD-Fw
413 (CACCATGGTGACCGGTACA) with CNluc-CTD_Rv (TCACTGGATGAATCCCATGTTG). The resulting entry
414 vectors were then recombined into destination vectors via Gateway™ LR Clonase™ II Enzyme mix
415 (Thermo-Fisher Scientific), to produce the desired expression constructs. A 35S:PLS-*crtW* construct for
416 constitutive transgene expression in plants was obtained by recombination of the proper entry vector,
417 containing the *crtW* coding sequence from *Agrobacterium aurantiacum* (*Paracoccus sp.* N81106), with
418 the binary vector pK7WG2 (Karimi, Inze and Depicker, 2002). The individual modules PLS-NTD-NNluc,
419 PLS-CNluc-CTD, NTD-NNluc and CNluc-CTD were, instead, recombined with the plasmid p2GW7 (Karimi,
420 Inze and Depicker, 2002), suitable for transient expression in Arabidopsis protoplasts.

421 **Protein structure modeling**

422 The three-dimensional structure of CNluc-CTD and NTD-NNluc was generated according the following
423 procedure: the amino acid sequences of both CNluc-CTD and NTD-NNluc were aligned to the template
424 sequences of Orange Carotenoid Protein of *Limnospira maxima* (PDB: 5UI2) (Kerfeld et al. 2003) and the
425 synthetic luciferase NanoLuc (PDB: 5IBO) (Lovell et al., unpublished) using MultAlin (Corpet, 1988) and
426 the resulting alignment used as input file for modeling using Modeller (Webb and Sali, 2016). Figure
427 rendering was performed with the PyMol software (DeLano, 2020).

428 **Plant materials and growth conditions**

429 Experiments were carried out using *Arabidopsis thaliana* accession Columbia (Col-0) as the wild-type
430 background. The *crtW* over-expressors were obtained exploiting *Agrobacterium tumefaciens*-mediated
431 transformation of the 35S:PLS-*crtW* construct in Col-0, following the floral dip protocol (Clough and
432 Bent, 1998). Transgenic seedlings were selected for resistance on kanamycin and subsequently verified
433 by PCR for the presence of the transgene with the following primers: attB1
434 (GGGACAAGTTTGTACAAAAAAGCAGGCT) and PLS_*crtW*_Rv (TCAGGCGGTATCACCTTAGT). Soil-grown
435 plants were cultivated at 23°C day/18°C night under neutral day photoperiod (12 light : 12 darkness) in
436 single 6 cm pots using a 3:1 soil : perlite mixture (with HAWITA tray substrate), after seed vernalization
437 at 4°C in the dark and germinated. The quantum irradiance was 80-100 $\mu\text{mol photons m}^{-2} \text{s}^{-1}$. For the *in*
438 *vitro* selection of transformed plants, seeds were surface sterilized using 70% (v/v) ethanol and 10%
439 (v/v) commercial bleach solution and then rinsed 5-7 times with sterile distilled water. Seeds were then

440 sown on solid sterile ½ strength MS medium [0.215% (w/v) Murashige-Skoog (MS) salts (Sigma-Aldrich),
441 0.8% agar (w/v), 0.5% (w/v) sucrose, pH 5.7]. Genomic DNA was extracted following the protocol
442 described by Edwards et al., 1991.

443 **RNA extraction and gene expression analysis by qRT-PCR**

444 For qRT-PCR analysis, total RNA was extracted from 4 weeks old plants as described by Kosmacz et al.,
445 2015. cDNA was synthesized from 1 µg of total RNA using the Maxima Reverse Transcriptase kit (Life
446 Technologies). Real-time PCR amplification was performed on 12.5 ng cDNA with the ABI Prism 7300
447 sequence detection system (Applied Biosystems), using the PowerUp™ SYBR® Green Master Mix
448 (Applied Biosystems). Ubiquitin10 (*At4g053290*) was exploited as the housekeeping gene. A pair of
449 specific primers was designed on the *crtW* gene sequence: sgCRTWfw (GGCACAACGCTCGTTCCTCT) and
450 sgCRTWrv (AAACGCCACCAAGGCACAGT).

451 **Plasmid DNA Purification**

452 Highly concentrated plasmid DNA required for protoplast transformation was extracted from 100-mL
453 bacterial culture (Luria-Bertani medium) supplemented with the appropriate antibiotic. Bacterial pellets
454 were extracted with an alkaline lysis protocol, according to Sambrook and Russell, 2001. Briefly, pellets
455 were sequentially resuspended in 2 mL of a buffer containing 50 mM Glucose, 25 mM Tris-HCl and 10
456 mM EDTA (pH 8), lysed in 4 mL of a buffer containing 0.2 M NaOH and and 1% (w/v) SDS and neutralized
457 in 3 mL of a buffer composed of 3 M potassium acetate in 11.5% (v/v) glacial acetic acid. Next, nucleic
458 acids were precipitated with an equal volume of isopropanol and then treated with RNase A (Sigma-
459 Aldrich) for 1 h at 37°C. Following polyethylene glycol (PEG) precipitation (13% [w/v] PEG 8000 dissolved
460 in 1.6 M NaCl), phenol : chloroform extraction was performed and nucleic acids were precipitated in
461 absolute ethanol, with the aid of ammonium acetate 0.6M. Final elution was in nuclease-free water.

462 **Protoplast isolation and transformation**

463 Arabidopsis mesophyll protoplasts were isolated and transformed according to Wu et al., 2009. They
464 were transfected with 4 µg of each effector plasmid and incubated in multiwell plates at 23°C in the dark
465 for 16 hours.

466 **Light treatment of transfected protoplasts**

467 Multiwell plates containing the transfected protoplasts were placed under led lamps, with the possibility
468 to change both light wavelength and intensity. Red (615-630 nm), green (515-530 nm), blue (465-480
469 nm) and white light were used in our experiments, testing an intensity range from 5 to 350 $\mu\text{mol m}^{-2} \text{s}^{-1}$.
470 For the reversion experiment the samples were transferred in darkness for 5 or 30 min before sampling.

471 **Luciferase Activity Quantification**

472 Protoplasts were flash frozen in liquid nitrogen and lysed by adding 30 μl of Passive Lysis Buffer
473 (Promega). NanoLuc activity was then measured using the Nano-Glo[®] Luciferase Assay (Promega)
474 following the manufacturer's instructions. Luminescence was detected with a tube Luminometer
475 (Berthold). NanoLuc measurements were normalized according to the total protein concentration of
476 each sample, determined by means of the Bio-Rad colorimetric assay[®], based on the Bradford dye-
477 binding method (Bradford, 1976).

478 **Extraction and quantification of carotenoid content**

479 Pigments were extracted from leaves with 80% acetone buffered with Na_2CO_3 and quantified by
480 reverse-phase HPLC as described in Perozeni et al. 2020. In particular a Jasco LC-4000 extrema HPLC
481 system equipped with a C18 column (Synergi 4u Hydro-RP 80A, Phenomenex, USA) was used. 15-min
482 gradient of ethyl acetate (0 to 100%) in acetonitrile-water-triethylamine (9:1:0.01, vol/vol/vol) at a flow
483 rate of 1.5 ml/min was used (Lagarde, Beuf and Vermaas, 2000) and pigment detection was conducted
484 with a Jasco 350–750 nm diode array detector. Keto-carotenoids peaks were identified by comparing
485 retention times and spectra to commercially available standards (CaroteNature GmbH) as reported in
486 Perozeni et al. 2020.

487 **Phenotypic Analysis**

488 To quantify the phenotypic parameters of interest in *crtW* plants, pots were imaged at 17, 21 and 24
489 days after germination with a LabScanalyzer (LemnaTec, GmbH, Aachen, Germany), and images were
490 taken and analysed as described by Ventura et al., 2020.

491 **Statistical analyses**

492 Significant variations between genotypes or treatments were statistically evaluated using Student's t-
493 test and ordinary one-way ANOVA with multiple comparisons. Curves were fit to the data with
494 linear/non-linear regression. All the analysis were performed with GraphPad Prism 9 for Windows 10.

495

496

Parsed Citations

Alcorta, J. et al. (2019) 'Fischerella thermalis: a model organism to study thermophilic diazotrophy, photosynthesis and multicellularity in cyanobacteria', *Extremophiles*. doi: 10.1007/s00792-019-01125-4.

Google Scholar: [Author Only](#) [Title Only](#) [Author and Title](#)

Andres, J., Blomeier, T. and Zurbriggen, M. D. (2019) 'Synthetic switches and regulatory circuits in plants', *Plant Physiology*. doi: 10.1104/pp.18.01362.

Google Scholar: [Author Only](#) [Title Only](#) [Author and Title](#)

Bai, C. et al. (2017) 'Reconstruction of the astaxanthin biosynthesis pathway in rice endosperm reveals a metabolic bottleneck at the level of endogenous β -carotene hydroxylase activity', *Transgenic Research*, 26(1), pp. 13–23. doi: 10.1007/s11248-016-9977-x.

Google Scholar: [Author Only](#) [Title Only](#) [Author and Title](#)

Bao, H. et al. (2017) 'Additional families of orange carotenoid proteins in the photoprotective system of cyanobacteria', *Nature Plants*, 3(July), pp. 1–11. doi: 10.1038/nplants.2017.89.

Google Scholar: [Author Only](#) [Title Only](#) [Author and Title](#)

Bondanza, M. et al. (2020) 'The Molecular Mechanisms of Photoactivation of Orange Carotenoid Protein Revealed by Molecular Dynamics', pp. 1–8. doi: 10.1021/jacs.0c10461.

Google Scholar: [Author Only](#) [Title Only](#) [Author and Title](#)

Bradford, M. M. (1976) 'A rapid and sensitive method for the quantitation of microgram quantities of protein utilizing the principle of protein-dye binding', *Analytical Biochemistry*. doi: 10.1016/0003-2697(76)90527-3.

Google Scholar: [Author Only](#) [Title Only](#) [Author and Title](#)

Chatelle, C. et al. (2018) 'A Green-Light-Responsive System for the Control of Transgene Expression in Mammalian and Plant Cells', *ACS Synthetic Biology*, 7(5), pp. 1349–1358. doi: 10.1021/acssynbio.7b00450.

Google Scholar: [Author Only](#) [Title Only](#) [Author and Title](#)

Choi, S. K. et al. (2005) 'Characterization of β -carotene ketolases, CrtW, from marine bacteria by complementation analysis in *Escherichia coli*', *Marine Biotechnology*, 7(5), pp. 515–522. doi: 10.1007/s10126-004-5100-z.

Google Scholar: [Author Only](#) [Title Only](#) [Author and Title](#)

Clough, S. J. and Bent, A. F. (1998) 'Floral dip: A simplified method for *Agrobacterium*-mediated transformation of *Arabidopsis thaliana*', *Plant Journal*. doi: 10.1046/j.1365-313X.1998.00343.x.

Google Scholar: [Author Only](#) [Title Only](#) [Author and Title](#)

Corpet, F. (1988) 'Multiple sequence alignment with hierarchical clustering', *Nucleic Acids Research*. doi: 10.1093/nar/16.22.10881.

Google Scholar: [Author Only](#) [Title Only](#) [Author and Title](#)

DeLano, W. L. (2020) 'The PyMOL Molecular Graphics System, Version 2.3', Schrödinger LLC.

Dixon, A. S. et al. (2016) 'NanoLuc Complementation Reporter Optimized for Accurate Measurement of Protein Interactions in Cells', *ACS Chemical Biology*, 11(2), pp. 400–408. doi: 10.1021/acscchembio.5b00753.

Google Scholar: [Author Only](#) [Title Only](#) [Author and Title](#)

Dominguez-Martin, M. A. and Kerfeld, C. A. (2019) 'Engineering the orange carotenoid protein for applications in synthetic biology', *Current Opinion in Structural Biology*, 57, pp. 110–117. doi: 10.1016/j.sbi.2019.01.023.

Google Scholar: [Author Only](#) [Title Only](#) [Author and Title](#)

Edwards, K., Johnstone, C. and Thompson, C. (1991) 'A simple and rapid method for the preparation of plant genomic DNA for PCR analysis', *Nucleic Acids Research*. doi: 10.1093/nar/19.6.1349.

Google Scholar: [Author Only](#) [Title Only](#) [Author and Title](#)

Gupta, S. et al. (2015) 'Local and global structural drivers for the photoactivation of the orange carotenoid protein', *Proceedings of the National Academy of Sciences of the United States of America*, 112(41), pp. E5567–E5574. doi: 10.1073/pnas.1512240112.

Google Scholar: [Author Only](#) [Title Only](#) [Author and Title](#)

Gutmann, A. (2011) 'The ethics of synthetic biology: Guiding principles for emerging technologies', *Hastings Center Report*. doi: 10.1002/j.1552-146X.2011.tb00118.x.

Google Scholar: [Author Only](#) [Title Only](#) [Author and Title](#)

Hall, M. P. et al. (2012) 'Engineered luciferase reporter from a deep sea shrimp utilizing a novel imidazopyrazinone substrate', *ACS Chemical Biology*, 7(11), pp. 1848–1857. doi: 10.1021/cb3002478.

Google Scholar: [Author Only](#) [Title Only](#) [Author and Title](#)

Hart, J. E. et al. (2019) 'Engineering the phototropin photocycle improves photoreceptor performance and plant biomass production', *Proceedings of the National Academy of Sciences of the United States of America*, 116(25), pp. 12550–12557. doi: 10.1073/pnas.1902915116.

Google Scholar: [Author Only](#) [Title Only](#) [Author and Title](#)

Karimi, M., Inze, D. and Depicker, A. (2002) 'GATEWAYTM vectors for *Agrobacterium*-mediated plant transformation', *Trends in Plant*

Science.

Kay Holt, T. and Krogmann, D. W. (1981) 'A carotenoid-protein from cyanobacteria', *BBA - Bioenergetics*. doi: 10.1016/0005-2728(81)90045-1.

Google Scholar: [Author Only](#) [Title Only](#) [Author and Title](#)

Kennedy, M. J. et al. (2010) 'Rapid blue-light-mediated induction of protein interactions in living cells', *Nature Methods*, 7(12), pp. 973–975. doi: 10.1038/nmeth.1524.

Google Scholar: [Author Only](#) [Title Only](#) [Author and Title](#)

Kerfeld, C. A. et al. (2003) 'The Crystal Structure of a Cyanobacterial Water-Soluble Carotenoid Binding Protein let chlorophyll, deexciting it in a preemptive reaction before singlet oxygen can be formed (reviewed in [1–3]). For example, transforming cyanobacteria with various', *Structure*, 11(02), pp. 55–65.

Google Scholar: [Author Only](#) [Title Only](#) [Author and Title](#)

Kirilovsky, D. and Kerfeld, C. A. (2013) 'The Orange Carotenoid Protein: A blue-green light photoactive protein', *Photochemical and Photobiological Sciences*, 12(7), pp. 1135–1143. doi: 10.1039/c3pp25406b.

Google Scholar: [Author Only](#) [Title Only](#) [Author and Title](#)

Kosmacz, M. et al. (2015) 'The stability and nuclear localization of the transcription factor RAP2.12 are dynamically regulated by oxygen concentration', *Plant, Cell and Environment*. doi: 10.1111/pce.12493.

Google Scholar: [Author Only](#) [Title Only](#) [Author and Title](#)

Lagarde, D., Beuf, L. and Vermaas, W. (2000) 'Increased production of zeaxanthin and other pigments by application of genetic engineering techniques to *Synechocystis* sp. strain PCC 6803', *Applied and Environmental Microbiology*. doi: 10.1128/AEM.66.1.64-72.2000.

Google Scholar: [Author Only](#) [Title Only](#) [Author and Title](#)

Lechno-Yossef, S. et al. (2017) 'Synthetic OCP heterodimers are photoactive and recapitulate the fusion of two primitive carotenoproteins in the evolution of cyanobacterial photoprotection', *Plant Journal*, 91(4), pp. 646–656. doi: 10.1111/tbj.13593.

Google Scholar: [Author Only](#) [Title Only](#) [Author and Title](#)

Leverenz, R. L. et al. (2014) 'Structural and functional modularity of the orange carotenoid protein: Distinct roles for the N- and C-terminal domains in cyanobacterial photoprotection', *Plant Cell*, 26(1), pp. 426–437. doi: 10.1105/tpc.113.118588.

Google Scholar: [Author Only](#) [Title Only](#) [Author and Title](#)

Leverenz, R. L. et al. (2015) 'A 12 Å carotenoid translocation in a photoswitch associated with cyanobacterial photoprotection', *Science*, 348(6242), pp. 1463–1466. doi: 10.1126/science.aaa7234.

Google Scholar: [Author Only](#) [Title Only](#) [Author and Title](#)

Merezhko, M. et al. (2020) 'Live-cell monitoring of protein localization to membrane rafts using protein-fragment complementation', *Bioscience Reports*, 40(1), pp. 1–13. doi: 10.1042/BSR20191290.

Google Scholar: [Author Only](#) [Title Only](#) [Author and Title](#)

'Method of the Year 2010' (2011) *Nature Methods*. doi: 10.1038/nmeth.f.321.

Google Scholar: [Author Only](#) [Title Only](#) [Author and Title](#)

Misawa, N. et al. (1995) 'Canthaxanthin biosynthesis by the conversion of methylene to keto groups in a hydrocarbon β -carotene by a single gene', *Biochemical and Biophysical Research Communications*. doi: 10.1006/bbrc.1995.1579.

Google Scholar: [Author Only](#) [Title Only](#) [Author and Title](#)

Möglich, A. et al. (2010) 'Structure and function of plant photoreceptors', *Annual Review of Plant Biology*. doi: 10.1146/annurev-arplant-042809-112259.

Google Scholar: [Author Only](#) [Title Only](#) [Author and Title](#)

Müller, K. et al. (2013) 'Multi-chromatic control of mammalian gene expression and signaling', *Nucleic Acids Research*, 41(12). doi: 10.1093/nar/gkt340.

Google Scholar: [Author Only](#) [Title Only](#) [Author and Title](#)

Nielsen, A. Z. et al. (2013) 'Redirecting photosynthetic reducing power toward bioactive natural product synthesis', *ACS Synthetic Biology*, 2(6), pp. 308–315. doi: 10.1021/sb300128r.

Google Scholar: [Author Only](#) [Title Only](#) [Author and Title](#)

Nisar, N. et al. (2015) 'Carotenoid metabolism in plants', *Molecular Plant*, 8(1), pp. 68–82. doi: 10.1016/j.molp.2014.12.007.

Google Scholar: [Author Only](#) [Title Only](#) [Author and Title](#)

Olson, E. J. and Tabor, J. J. (2014) 'Optogenetic characterization methods overcome key challenges in synthetic and systems biology', *Nature Chemical Biology*. doi: 10.1038/nchembio.1559.

Google Scholar: [Author Only](#) [Title Only](#) [Author and Title](#)

Paik, I. and Huq, E. (2019) 'Plant photoreceptors: Multi-functional sensory proteins and their signaling networks', *Seminars in Cell and Developmental Biology*. doi: 10.1016/j.semcdb.2019.03.007.

Google Scholar: [Author Only](#) [Title Only](#) [Author and Title](#)

Perozeni, F. et al. (2020) 'Turning a green alga red: engineering astaxanthin biosynthesis by intragenic pseudogene revival in *Chlamydomonas reinhardtii*', Plant Biotechnology Journal. doi: 10.1111/pbi.13364.

Google Scholar: [Author Only Title Only Author and Title](#)

Pouvreau, B. et al. (2020) 'A Versatile High Throughput Screening Platform for Plant Metabolic Engineering Highlights the Major Role of ABI3 in Lipid Metabolism Regulation', Frontiers in Plant Science. doi: 10.3389/fpls.2020.00288.

Google Scholar: [Author Only Title Only Author and Title](#)

Punginelli, C. et al. (2009) 'Influence of zeaxanthin and echinenone binding on the activity of the Orange Carotenoid Protein', Biochimica et Biophysica Acta - Bioenergetics, 1787(4), pp. 280–288. doi: 10.1016/j.bbabi.2009.01.011.

Google Scholar: [Author Only Title Only Author and Title](#)

Ruiz-Sola, M. Á and Rodríguez-Concepción, M. (2012) 'Carotenoid Biosynthesis in Arabidopsis: A Colorful Pathway', The Arabidopsis Book, 10, p. e0158. doi: 10.1199/tab.0158.

Google Scholar: [Author Only Title Only Author and Title](#)

Sambrook, J. and Russell, D. W. (2001) 'Molecular Cloning: A Laboratory Manual, Third Edition', in Molecular Cloning: a laboratory a manual.

Sineshchekov, O. A, Jung, K. H. and Spudich, J. L. (2002) 'Two rhodopsins mediate phototaxis to low- and high-intensity light in *Chlamydomonas reinhardtii*', Proceedings of the National Academy of Sciences of the United States of America. doi: 10.1073/pnas.122243399.

Google Scholar: [Author Only Title Only Author and Title](#)

Sun, T. et al. (2018) 'Carotenoid Metabolism in Plants: The Role of Plastids', Molecular Plant. doi: 10.1016/j.molp.2017.09.010.

Google Scholar: [Author Only Title Only Author and Title](#)

Tilbrook, K. et al. (2013) 'The UVR8 UV-B Photoreceptor: Perception, Signaling and Response', The Arabidopsis Book. doi: 10.1199/tab.0164.

Google Scholar: [Author Only Title Only Author and Title](#)

Ventura, I. et al. (2020) 'Arabidopsis phenotyping reveals the importance of alcohol dehydrogenase and pyruvate decarboxylase for aerobic plant growth', Scientific Reports. doi: 10.1038/s41598-020-73704-x.

Google Scholar: [Author Only Title Only Author and Title](#)

Verhounig, A., Karcher, D. and Bock, R. (2010) 'Inducible gene expression from the plastid genome by a synthetic riboswitch', Proceedings of the National Academy of Sciences of the United States of America, 107(14), pp. 6204–6209. doi: 10.1073/pnas.0914423107.

Google Scholar: [Author Only Title Only Author and Title](#)

Wang, F. Z et al. (2020) 'Split Nano luciferase complementation for probing protein-protein interactions in plant cells', Journal of Integrative Plant Biology, 62(8), pp. 1065–1079. doi: 10.1111/jipb.12891.

Google Scholar: [Author Only Title Only Author and Title](#)

Webb, B. and Sali, A. (2016) 'Comparative protein structure modeling using MODELLER', Current Protocols in Bioinformatics. doi: 10.1002/cpbi.3.

Google Scholar: [Author Only Title Only Author and Title](#)

Wilson, A. et al. (2006) 'A soluble carotenoid protein involved in phycobilisome-related energy dissipation in cyanobacteria', Plant Cell, 18(4), pp. 992–1007. doi: 10.1105/tpc.105.040121.

Google Scholar: [Author Only Title Only Author and Title](#)

Wilson, A. et al. (2008) 'A photoactive carotenoid protein acting as light intensity sensor', Proceedings of the National Academy of Sciences of the United States of America, 105(33), pp. 12075–12080. doi: 10.1073/pnas.0804636105.

Google Scholar: [Author Only Title Only Author and Title](#)

Wilson, A. et al. (2011) 'Essential role of two tyrosines and two tryptophans on the photoprotection activity of the Orange Carotenoid Protein', Biochimica et Biophysica Acta - Bioenergetics, 1807(3), pp. 293–301. doi: 10.1016/j.bbabi.2010.12.009.

Google Scholar: [Author Only Title Only Author and Title](#)

Wu, F. H. et al. (2009) 'Tape-arabidopsis sandwich - A simpler arabidopsis protoplast isolation method', Plant Methods. doi: 10.1186/1746-4811-5-16.

Google Scholar: [Author Only Title Only Author and Title](#)

Wu, Y. P. and Krogmann, D. W. (1997) 'The orange carotenoid protein of *Synechocystis* PCC 6803', Biochimica et Biophysica Acta - Bioenergetics, 1322(1), pp. 1–7. doi: 10.1016/S0005-2728(97)00067-4.

Google Scholar: [Author Only Title Only Author and Title](#)

Xiang, N. et al. (2020) 'Erratum: Using synthetic biology to overcome barriers to stable expression of nitrogenase in eukaryotic organelles (Proceedings of the National Academy of Sciences of the United States of America (2020) 117 (16537-16545) DOI: 10.1073/pnas.2002307117)', Proceedings of the National Academy of Sciences of the United States of America, 117(39), p. 24602. doi: 10.1073/pnas.2017731117.

Google Scholar: [Author Only Title Only Author and Title](#)

Yazawa, M. et al. (2009) 'Induction of protein-protein interactions in live cells using light', *Nature Biotechnology*, 27(10), pp. 941–945. doi: 10.1038/nbt.1569.

Google Scholar: [Author Only](#) [Title Only](#) [Author and Title](#)

Yoo, S. D., Cho, Y. H. and Sheen, J. (2007) 'Arabidopsis mesophyll protoplasts: A versatile cell system for transient gene expression analysis', *Nature Protocols*. doi: 10.1038/nprot.2007.199.

Google Scholar: [Author Only](#) [Title Only](#) [Author and Title](#)

Zhong, Y. J. et al. (2011) 'Functional characterization of various algal carotenoid ketolases reveals that ketolating zeaxanthin efficiently is essential for high production of astaxanthin in transgenic Arabidopsis', *Journal of Experimental Botany*. doi: 10.1093/jxb/err070.

Google Scholar: [Author Only](#) [Title Only](#) [Author and Title](#)